iScience

CellPress
OPEN ACCESS

Article

Single cell *in vivo* optogenetic stimulation by two-photon excitation fluorescence transfer

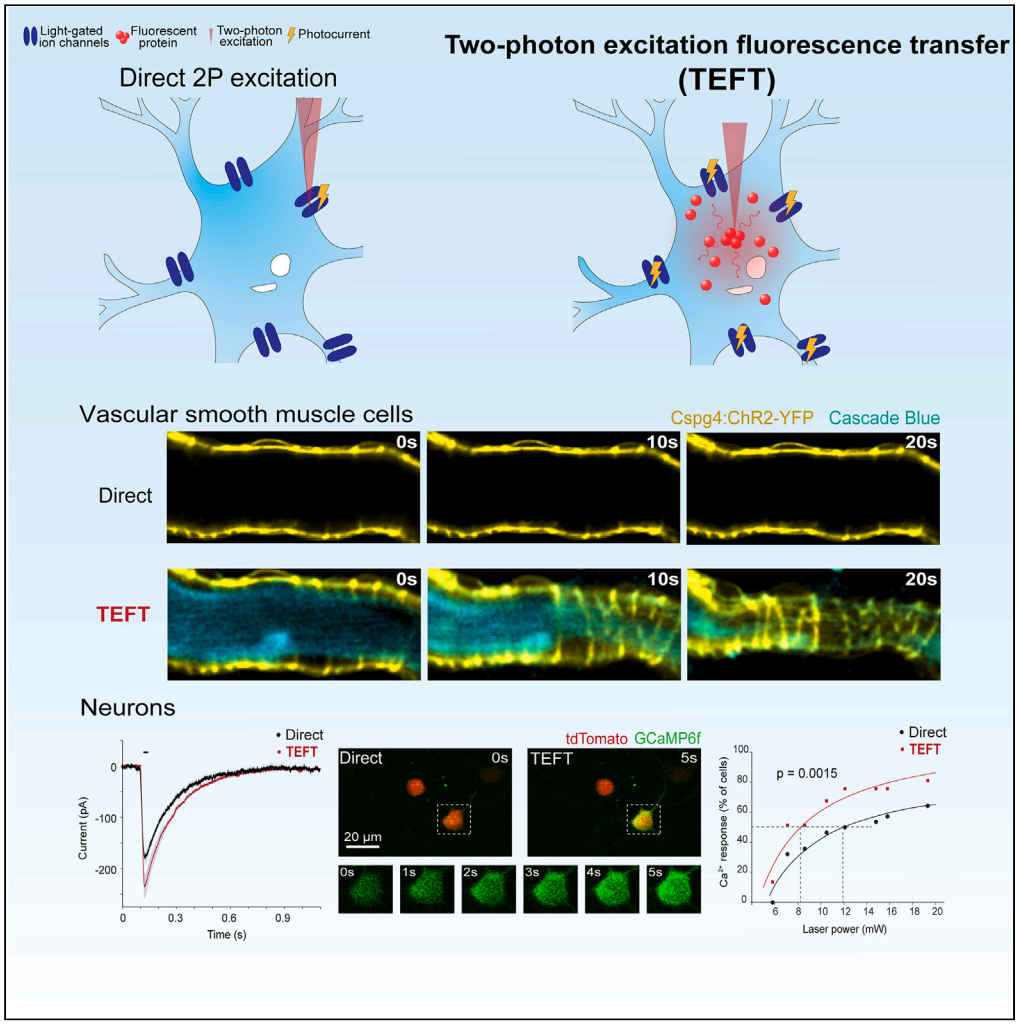

Lei Tong, Shanshan Han, Yao Xue, ..., Z. Jimmy Zhou, Peng Yuan, Jaime Grutzendler

pyuan@fudan.edu.cn (P.Y.)
jaime.grutzendler@yale.edu (J.G.)

Highlights

A new principle for optogenetics by two-photon excitation fluorescence transfer (TEFT)

TEFT facilitates optogenetic control of individual blood vessels *in vivo*

TEFT improves the efficiency of 2P optogenetics for neuronal activation *in vivo*

We provide a theoretical framework for TEFT fluorophore optimization

Tong et al., iScience *26*, 107857
October 20, 2023 © 2023 The Authors.
https://doi.org/10.1016/j.isci.2023.107857

iScience

CellPress
OPEN ACCESS

Article

Single cell *in vivo* optogenetic stimulation by two-photon excitation fluorescence transfer

Lei Tong,[1] Shanshan Han,[2] Yao Xue,[3] Minggang Chen,[3] Fuyi Chen,[1] Wei Ke,[8] Yousheng Shu,[8] Ning Ding,[2] Joerg Bewersdorf,[5,6] Z. Jimmy Zhou,[3,4,7] Peng Yuan,[1,2,*] and Jaime Grutzendler[1,4,9,*]

SUMMARY

Optogenetic manipulation with single-cell resolution can be achieved by two-photon excitation. However, this frequently requires relatively high laser powers. Here, we developed a novel strategy that can improve the efficiency of current two-photon stimulation technologies by positioning fluorescent proteins or small fluorescent molecules with high two-photon cross-sections in the vicinity of opsins. This generates a highly localized source of endogenous single-photon illumination that can be tailored to match the optimal opsin absorbance. Through neuronal and vascular stimulation in the live mouse brain, we demonstrate the utility of this technique to achieve efficient opsin stimulation, without loss of cellular resolution. We also provide a theoretical framework for understanding the potential advantages and constrains of this methodology, with directions for future improvements. Altogether, this fluorescence transfer illumination method opens new possibilities for experiments difficult to implement in the live brain such as all-optical neural interrogation and control of regional cerebral blood flow.

INTRODUCTION

Optogenetics with light-sensitive opsins has revolutionized the field of neuroscience.[1] Typical experiments involve the utilization of single-photon illumination of the brain to activate opsins such as channelrhodopsin (ChR2) and others.[2] While this allows temporally precise manipulation of cell ensembles, all the cells along the conical illumination light path are activated, reducing the spatial specificity, and resulting in artificially synchronized activity patterns.[3] These drawbacks limit the application of optogenetics to answer important questions involving manipulation of specific cells such as neurons and other excitable cells like vascular smooth muscle cells (vSMC) and astrocytes, within ensembles. In order to overcome these limitations, it is desirable to achieve optogenetic stimulation with single-cell level precision. One approach is to utilize two-photon absorption, which is characterized by being limited to the immediate vicinity of the focal point, thereby achieving spatially restricted activation of opsin channels.[3] Several studies have demonstrated the feasibility of this approach[4–12]; however, two-photon optogenetics has relatively low efficiency in eliciting a biological response, which limits *in vivo* applications (Figure S1).

One of the reasons for its low efficiency is that the two-photon effect occurs in a submicron focal volume.[13] Thus, only a small patch of cell membrane is illuminated at any point in time during laser scanning, which limits the number of opsin molecules that are synchronously stimulated. This limits the ion flux necessary to induce changes in membrane potential and the resulting ability to trigger action potentials. Opsin stimulation can be improved using higher laser power, but this can have undesirable effects on membrane potential and cell excitability,[14–16] likely due to two-photon thermal effects,[17,18] which can cause confounding opsin- or activity-independent ion channel opening. Furthermore, the use of high laser power is problematic as it may induce a variety of cell signaling changes and toxicity.[19–21] An alternative to improve the efficiency of two-photon illumination is to use fast laser scanning and generate spiral paths that roughly match the cell's perimeter, which allows nearly simultaneous activation of a larger number of opsin channels along the cellular membrane.[4,9] A related technique uses spatial light modulators to generate a hologram in the sample so that the laser can simultaneously illuminate the entire target cell[12,22,23] and thereby elicit a more robust cellular response. While studies have demonstrated *in vivo* manipulation of neural activity at single-cell resolution with both techniques,[24–27] they require advanced optics and complex instrument operation that limit their implementation by

[1]Department of Neurology, Yale School of Medicine, New Haven, CT 06511, USA
[2]Department of Rehabilitation Medicine, Huashan Hospital, State Key Laboratory of Medical Neurobiology, Institute for Translational Brain Research, MOE Frontiers Center for Brain Science, Fudan University, Shanghai 200032, China
[3]Department of Ophthalmology and Visual Science, Yale School of Medicine, New Haven, CT 06511, USA
[4]Department of Neuroscience, Yale School of Medicine, New Haven, CT 06511, USA
[5]Department of Cell Biology, Yale School of Medicine, New Haven, CT 06511, USA
[6]Department of Biomedical Engineering, Yale University, New Haven, CT 06511, USA
[7]Department of Cellular and Molecular Physiology, Yale University, New Haven, CT 06511, USA
[8]Department of Neurology, Huashan Hospital, State Key Laboratory of Medical Neurobiology, Institute for Translational Brain Research, MOE Frontiers Center for Brain Science, Fudan University, Shanghai 200032, China
[9]Lead contact
*Correspondence: pyuan@fudan.edu.cn (P.Y.), jaime.grutzendler@yale.edu (J.G.)
https://doi.org/10.1016/j.isci.2023.107857

This is an open access article under the CC BY-NC-ND license (http://creativecommons.org/licenses/by-nc-nd/4.0/).

most researchers. Thus, it would be of great utility to improve the efficiency by which opsins are stimulated with conventional two-photon illumination and thereby achieve reduced laser scanning times and power requirements. Here we propose a robust and practical approach to achieve *in vivo* optogenetic control of single cells that we termed two-photon excitation fluorescence transfer (TEFT). This approach has the potential to markedly improve the efficiency of targeted optogenetic control of excitable cells in the live brain and is entirely compatible with current methodologies including spiral cell scanning and holographic illumination, commonly used for studies of brain networks, cell physiology and neurovascular coupling.

RESULTS

Two-photon excitation fluorescence transfer (TEFT) for *in vivo* optogenetics

In conventional two-photon optogenetics, opsins located in a small patch of membrane defined by the width of the diffraction-limited point-spread-function (PSF) (hundreds of nanometers diameter) are activated at any point in time, leading to relatively inefficient stimulation of the cell.[9] Instead of directly activating the light-sensitive opsin channels on the cell membrane, TEFT utilizes the two-photon laser to excite fluorophores or organic dyes in the vicinity of opsins. These fluorophores have a fluorescence emission spectrum matching the optimal (single-photon) opsin absorption, which is now used instead of two-photon excitation to indirectly stimulate opsins in the target cell and generate photocurrents (Figure S1). In contrast to the direct two-photon excitation in which the laser power is only effective when focused on the cell membrane, TEFT utilizes the laser power during the entire scanning period and converts the laser energy that does not focus on membrane into single-photon emission that can activate the opsin. The same principle is applicable in two-photon stimulation techniques using spiral scan or holographic illumination, as TEFT harnesses additional laser energy that is not directly absorbed by the opsins (Figure S1C).

Effectively, TEFT converts two-photon stimulation into a local single-photon point source that can be used for optogenetics. Two predispositions may affect the efficiency of TEFT: firstly, the fluorophore's maximal emission wavelength should be close to the opsin's maximal absorption wavelength; and secondly high two-photon cross-section and quantum yield of the fluorophore and high photocurrents of the opsin are preferable. Taken these into consideration, we chose the tdTomato-ReaChR pair and calculated the energy of fluorescence light, in order to understand the efficiency of the TEFT process (Figure 1). We calculated the number of fluorescence photons that are emitted per pulse from a single tdTomato protein under different two-photon excitation wavelengths (Figures 1B and 1C). We then calculated the focal volume for different numerical aperture objective configurations at 1050 nm (Figures 1D and 1E). The product from the above two sets of calculations allowed us to estimate the total fluorescence flux of TEFT excitation (Figure 1F). Note that the total fluorescence flux is approximately independent of numerical aperture (Figure S2). Thus, we could calculate the fluorescence irradiance to the cell surface assuming a standard shape and size of the cell (Figure 1G). We estimated that with a laser power of 20 mW, the TEFT excitation would generate a fluorescence irradiance of 0.075 mW/mm^2. Based on the *in vitro* measurements from previous work,[28] such single-photon excitation could generate a photocurrent around 80 pA at steady state, which could be sufficient to induce action potential in neurons, and is at the same order of magnitude as the amount of currents induced by other two-photon optogenetic methods.[28,29] In conclusion, our calculation indicated that TEFT-based excitation could in theory generate sufficient illumination to activate optogenetic ion channels.

To ensure the accuracy of the two-photon excitation we estimate the excitation ratio of the neighbor cell and the target cell at different distances, the excitation ratio decreases with increasing distance until it reaches approximately zero at 10 μm (Figure S4A). We have also estimated the potential illumination ratios of the neighbor cell at various sizes and distances from the target cell because there may be two cells with different sizes. As the radius of the neighbor cell increases and the distance to the target cell become closer, the illumination ratio rises (Figure S4B), but never exceeds 14%. Thus, we provided theoretical calculations demonstrating the ability to retain single cell resolution with TEFT excitation.

In vivo optogenetic control of vascular smooth muscle cells with TEFT stimulation

Guided by the abovementioned TEFT optogenetics principles, we tested the feasibility of two-photon optogenetic stimulation of vSMC in the live mouse brain to locally control cerebral blood flow.[30] Optogenetic control of the brain vasculature has recently been implemented as a powerful tool for dissecting mechanisms of neurovascular coupling and its control by different vascular mural cell types.[31–33] We hypothesized that TEFT may improve the efficiency and reliability of vascular optogenetics, and thus investigated this method with various combinations of opsins and intravascular fluorescent dyes as previously described.[34] We first tested the ability to induce vessel constriction in Cspg4-Ai32 mice, in which the perivascular vSMCs express the excitatory ChR2. In order to provide the fluorescence emission that matches the optimal absorption of ChR2, we intravascularly injected cascade blue-conjugated albumin. We then scanned a region of interest (ROI) over the selected vessel segment using the femtosecond laser tuned to 800 nm, a wavelength that is suboptimal to directly excite ChR2[35] and therefore cannot induce adequate vSMC contraction (Figure 2). As predicted, we observed a robust vessel constriction that was only elicited when we implemented the stimulation in the presence of intravascular cascade blue (Figure 2A, Video S1). In contrast, we did not observe any vessel constriction when we used an unconjugated control albumin, albumin conjugated with a dye not optimally matched to ChR2 absorption (Figure S3) or when we used a 950-nm wavelength, which does not excite the cascade blue dye (Figure 2E). Importantly, the stimulation only induced constriction of the targeted vessel segments, while the diameter of adjacent segments or vessels in the nearby region remained unchanged (Figures 2F and S4), demonstrating the spatial precision of this technique. Next, we used archaerhodopsin (Arch)-expressing mice (Cspg4-ArchT (Ai40D)) to induce vSMC hyperpolarization and determine the efficiency of TEFT to induce vSMC-relaxation and consequent vasodilation. To achieve the optimal single-photon activation wavelength of Arch (~545 nm[36]), we utilized an intravascular Alexa 514-conjugated albumin. This resulted in efficient and focal vessel dilation (Video S2), which did not occur in the absence of the intravascular

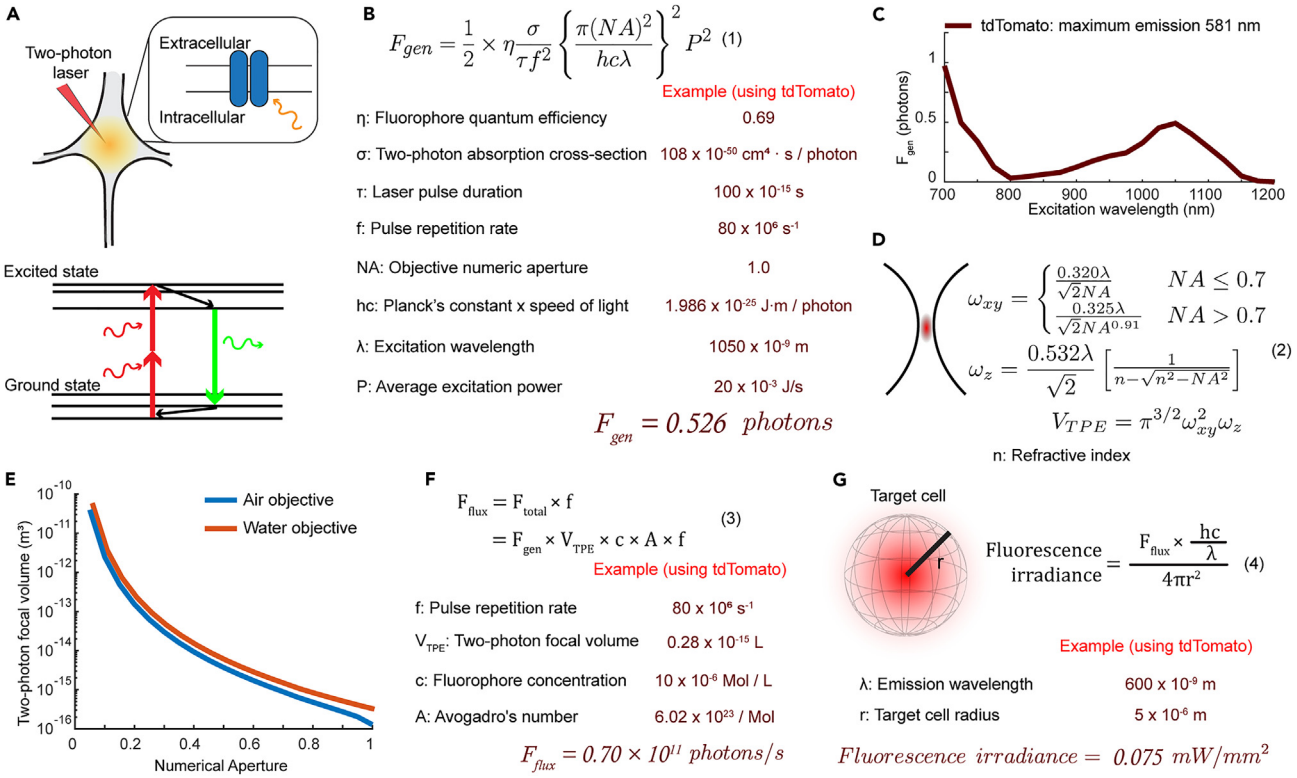

Figure 1. Theoretical estimation of fluorescence irradiance with two-photon excitation

(A) Schematic diagram of fluorescence transfer mediated two-photon optogenetics and the Jablonski diagram for the principle of two-photon excitation. Two-photon excitation generates fluorescence that can be absorbed by opsins expressed on the cell membrane. Two prerequisites for efficient fluorescence transfer optogenetics: 1, matching the spectrum between fluorophore emission and opsin absorption; and 2, sufficient irradiance of the fluorescence to generate photocurrents.

(B) Equations describing the photons generated per fluorophore per pulse (modified from previous work[13,49]). In our simulated condition, the absorption will be saturated (1 photon per molecule per pulse) when laser power exceeds 27.5 mW. At energy below this level, saturation is neglected.

(C) Simulation of two-photon excited fluorescent photon for tdTomato at different excitation wavelengths.

(D) Equations estimating two-photon focal volume (modified from previous work[50]).

(E) Theoretical calculation of two-photon focal volume at 1050 nm, with air or water objective at different numerical aperture configurations.

(F) Equations estimating total fluorescence flux.

(G) Equations estimating fluorescence irradiance to the cell surface.

dye (Figures 2G and 2H). For both ChR2 and ArchT activation, we found that many other dyes with similar emissions were capable of inducing opsin activation. For example, all three blue-emitting fluorescent dyes, Cascade-blue, Alexa 405 and AMCA (aminomethylcoumarin acetate), were able to trigger vessel contraction in Cspg4-ChR2 mice (Figure 2I), while the two yellow-emitting dyes, Alexa 514 and Lucifer yellow, produced vessel dilation in Cspg4-ArchT mice (Figure 2J). Together, these results demonstrate that the fluorescence generated from these intravascular dyes by two-photon excitation was a potent indirect light source for highly efficient and spatially restricted optogenetic control of vSMCs *in vivo*.

TEFT provides sufficient two-photon optogenetic activation in neurons

Having demonstrated the effectiveness of TEFT using intravascular dyes to activate vSMCs, we next explored the feasibility of applying this method to neurons. In order to measure the efficiency of optogenetics, we performed patch-clamp recordings of pyramidal neurons in acute mouse brain slices (Figure 3). We implemented TEFT, by expressing ReaChR in neurons (through *in utero* electroporation) and filling the recording electrode with Alexa 594 solution (Figure 3A). To achieve optogenetic stimulation, we scanned these cells by two-photon illumination of an ROI covering the entire cell body using a wavelength of 800 nm for ~50 ms. We found that adding the dye increased the peak current by ~50%, compared to cells with no dye, under the same laser stimulation conditions (Figures 3B and 3C). In addition, TEFT-mediated activation showed faster onset kinetics compared to direct two-photon optogenetics (Figure 3D), consistent with the TEFT principle, that all opsins on the target cell were activated simultaneously (Figure S1), rather than sequentially as is the case with direct two-photon membrane-opsin activation.

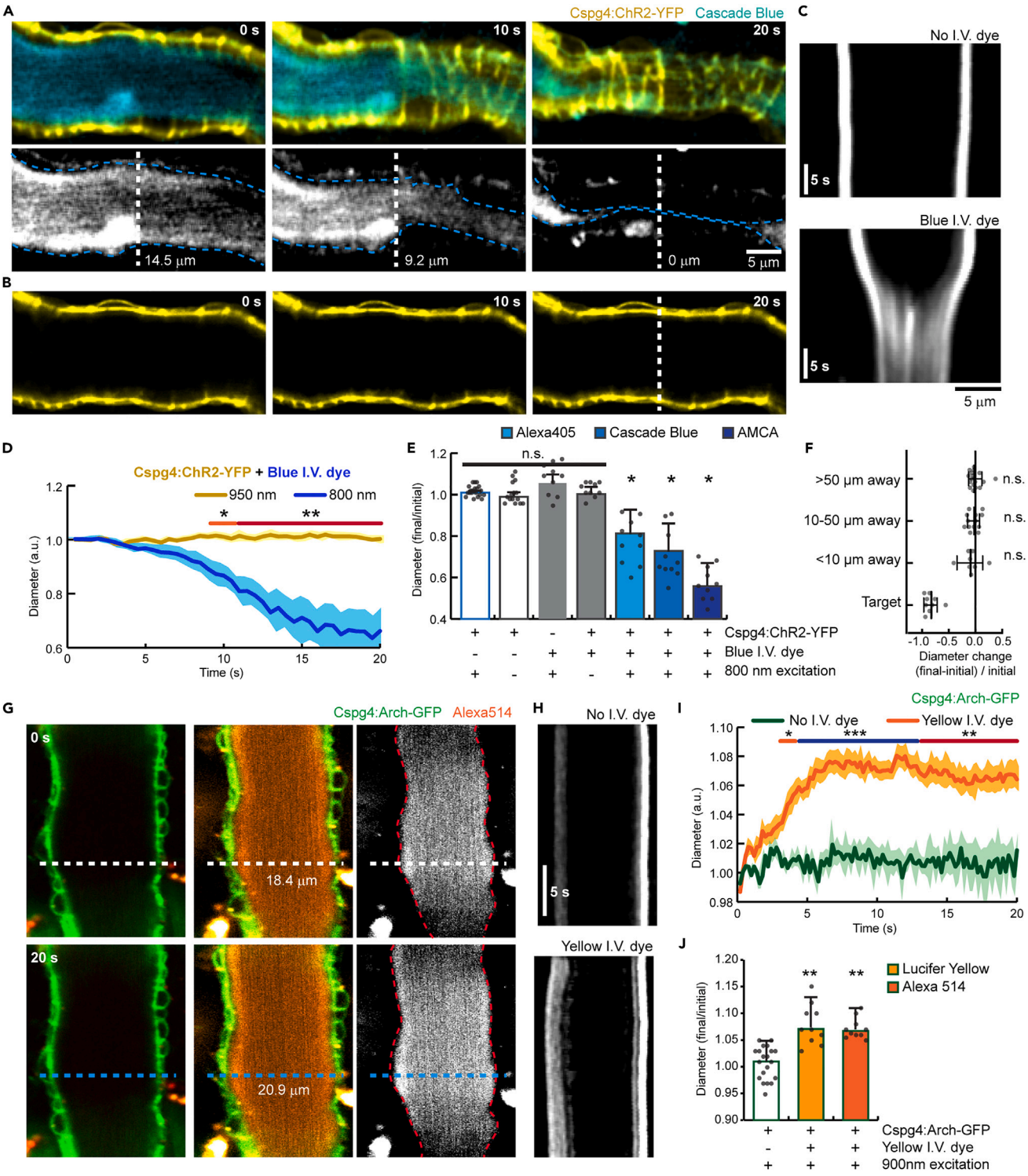

Figure 2. Fluorescence transfer-mediated two-photon optogenetic control of vascular smooth muscle cells *in vivo*

(A) Time-lapse intravital brain imaging in mice expressing ChR2 in vascular smooth muscle cells (Cspg4:ChR2-YFP) show focal vessel constriction induced by two-photon illumination of intravascular blue dye (cascade blue). Blue dashed lines (lower row) show the outlines of the intravascular space (cross-section widths indicated by white dashed lines).

(B) Time-lapse images of the same vessel segment as in a, without the intravascular blue dye, showing no changes in diameter with the same laser power. Scanning parameters in a and b: 25 Hz, 800 nm laser, 10 µs dwell time, 10mW.

Figure 2. *Continued*

(C) Vessel cross-sections during the scanning periods at the locations of white dashed lines in a and b.

(D) Quantification of normalized vessel diameters during two-photon scanning at 800nm and 950nm wavelengths. Data are represented as mean ± standard deviation. N = 10 vessels for each group. Orange and red segments indicate statistically significant timepoints between groups (*: $p < 0.05$ and **: $p < 0.01$, respectively, Student's *t* test between groups for each time points, with Bonferroni's correction for multiple comparisons).

(E) Quantifications of vessel diameters at the end of the stimulation with different experimental conditions. Data are presented as mean ± standard deviation, with individual datapoints provided (N = 10 to 20 vessels per group). One sample Wilcoxon tests were used for each group to compare to 1, with additional Bonferroni's correction for multiple comparisons (*: $p < 0.05$).

(F) Quantification of vessel diameter changes between the start and the end of TEFT stimulation in the vessel segments at different distances to the target region. Data are presented as mean ± standard deviation, with individual datapoints provided (N = 10 to 20 vessels per group). One sample Wilcoxon tests were used for each group to compare to 0.

(G) Representative two-photon time-lapse images of vessel dilation in archaerhodopsin expressing mouse (Cspg4:ArchT-GFP). White and blue dashed lines show site where diameter was measure. Scanning parameters in g: 25 Hz, 900 nm laser, 10 μs dwell time, 10mW.

(H) Vessel cross-section line profiles depicted overtime during scanning at the locations of dashed lines in g.

(I) Quantification of normalized vessel diameters with and without yellow intravascular dye. Data are represented as mean ± standard deviation. N = 10 vessels per group. Yellow, red and blue segments indicate statistically significant timepoints between groups (*: $p < 0.05$; **: $p < 0.01$ and ***: $p < 0.001$, respectively, Student's *t* test between groups for each time point, with Bonferroni's correction for multiple comparison).

(J) Quantification of vessel diameters with different experimental conditions. Data are presented as mean ± standard deviation, with individual datapoints provided. N = 10 to 20 vessels per group. One sample Wilcoxon tests were used for each group to compare to 1, with additional Bonferroni's correction for multiple comparison (**: $p < 0.01$). In all experiments, the dye concentration was about 0.5 mM.

We next applied TEFT in the live brain. Due to the difficulty of introducing organic fluorescent dyes into cells *in vivo*, we instead overexpressed fluorescent proteins in the target neurons. We used *in utero* electroporation of neurons in the mouse brain to first co-express the red-emitting fluorescent protein tdTomato and the opsin ReaChR (peak absorption 595 nm), as well as the calcium sensor GCaMP6 to detect neuronal activity changes. To test the feasibility of implementing TEFT in neurons, we scanned these cells by two-photon illumination of a ROI covering the entire cell body using a wavelength of 920 nm, which has been reported to excite ReaChR.[29] This focused scanning triggered a rise in GCaMP6 fluorescence (Figures 3E and 3F). The rising phase of the GCaMP fluorescence was relatively slow compared to the time required for action potentials. To better characterize the relationship between GCaMP signal and neuron activity, we performed simultaneous recording of membrane potentials and GCaMP imaging in acute brain slices (Figure S5). Consistent with previous reports,[37] we found that the rising phase of the fluorescence corresponded to the duration of action potential bursts, during which the intensity continued to increase, in proportion to the number of action potentials (Figure S5D).

We then compared this optogenetic-induced calcium rise in cells with and without tdTomato co-expression. While two-photon scanning can directly stimulate ReaChR at relatively high powers,[29] co-expression with tdTomato markedly increased the efficiency, and enabled activation with laser powers that are normally too low for ReaChR stimulation (Figure 3G). We observed ~30% reduction of the laser power required to reach 50% probability of activation using the TEFT method (Figure 3H). We then excited one of the two adjacent cells co-expressing ReaChR, GCaMP6 and tdTomato with 920nm excitation light. Importantly, TEFT improves the efficiency of cell activation while maintaining the single-cell resolution, since we could elicit a robust calcium rise in the targeted cell, without any calcium changes in the immediately adjacent ones (Figure S4). Together, these observations demonstrate that TEFT-mediated two-photon optogenetics improves the efficiency of neuronal activation.

Fluorophore/opsin constraints critical for optimal TEFT efficiency

In contrast to the tdTomato/ReaChR pair for TEFT optogenetic stimulation, we were not able to elicit two-photon activation of ChR2 when pairing it with genetically encoded blue fluorescent proteins or SNAPTag-targeted organic dyes co-expressed in the same neurons (Figure S6). This contrasts with the highly efficient activation we observed when ChR2 in vSMCs was stimulated in the presence of blue intravascular small organic dyes (Figure 2). As an explanation for this phenomenon, we hypothesized that the number of photons emitted by the donor fluorophores in the vicinity of opsins is a critical variable that determines their efficient activation. To better understand this relationship, we calculated the theoretical number of photons emitted after two-photon excitation of various well-known fluorescent proteins[38,39] (Figure S6). With these data, we determined that the mTagBFP/ChR2 pair that we used experimentally for neurons, was not suitable for TEFT optogenetics, given that for laser powers of ~10 mW, typical of most intravital applications, the calculated emitted fluorescence of mTagBFP was only of the order of 0.01 mW/mm^2, which is two orders of magnitude lower than the reported power needed for ChR2 activation.[40] In contrast, with the tdTomato/ReaChR pair, using 20 mW for two-photon illumination, yielded around 0.075 mW/mm^2 (Figure S6D), which is known to be sufficient to elicit strong ReaChR photocurrents.[28] One way to overcome the low two-photon cross section of most genetically encoded blue fluorescent proteins, would be to increase their intracellular concentration to achieve greater net photon emissions. However, it is difficult to increase their intracellular concentrations beyond ~10 μM.[41] This contrasts with the concentration of intravascular dyes that we used for stimulation of ChR2 in vSMCs (~500 μM), which can be further increased as needed, thereby achieving highly efficient TEFT optogenetic stimulation.

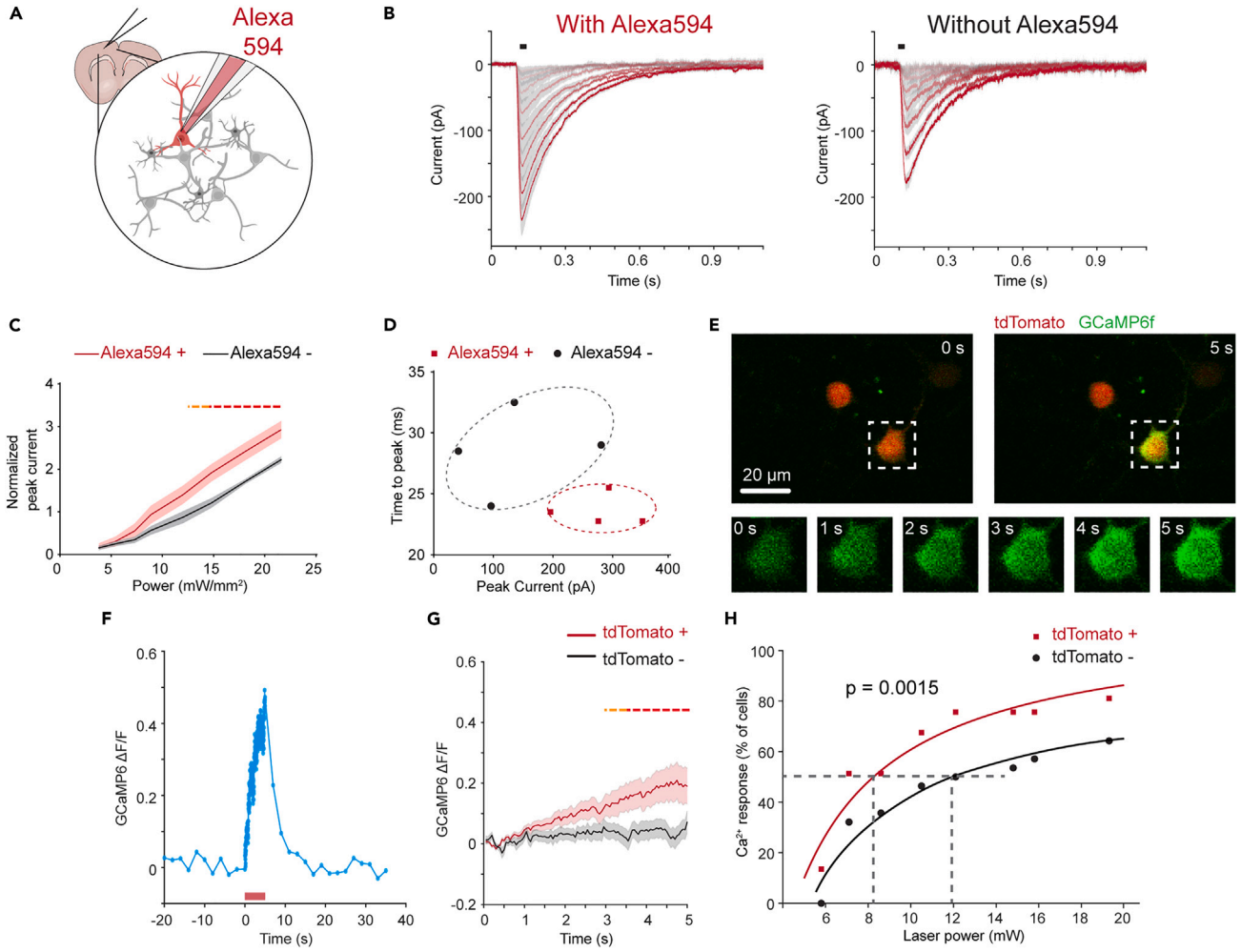

Figure 3. Optogenetics of single neurons using fluorescence transfer-mediated two-photon stimulation

(A) Schematics of patch clamp recording with TEFT.

(B) Representative traces of two-photon elicited currents in cells with or without Alexa 594 dye (0.5 mM) at 800 nm. Laser powers are 3.8, 5.4, 7.3, 8.9, 12, 14.8, 18.1 and 21.6 mW, for curves from gray color to red. Black lines indicate a 50 ms two-photon stimulation period.

(C) Quantification of the peak current amplitudes in cells with or without Alexa 594 dye, normalized by the peak current recorded at 920 nm at 5 mW. N = 4 cells in each group. Data are represented as mean ± standard error (Student's *t* test comparison between groups for each time point, a false discovery rate of 5% was set for multiple comparison correction. Yellow dash lines: $p < 0.05$, red dash lines: $p < 0.001$).

(D) Quantification of onset phase kinetics of two-photon activated currents in cells with or without Alexa 594 dye, plotted against peak currents. Dash lines indicate the perimeter for each condition group.

(E) Two-photon raster scanning in a live mouse brain of ROI (white dashed square) covering a neuron that is co-expressing ReaChR, GCaMP6 and tdTomato, induces robust calcium transients (ROI scan parameters: pixel size: 0.42 μm/pixel, 50 Hz, 5 s, 920 nm laser, 4 μs dwell time, 8.6 mW). Time-lapse images (bottom panel, green) show rapid increase in calcium levels following two-photon illumination.

(F) GCaMP6 calcium response of a neuron coexpressing ReaChR, GCaMP6 and tdTomato using the same scanning parameters as in e (ROI scanning interval indicated by the orange bar).

(G) Comparison of two-photon optogenetics in ReaChR/GCaMP6 positive neurons with and without tdTomato expression at 8.6 mW excitation power (N = 37 for tdTomato positive; N = 28 for tdTomato negative). Data are represented as mean ± standard error (Student's *t* test comparison between groups for each time point, a false discovery rate of 5% was set for multiple comparison correction. Yellow dash lines: $p < 0.05$, red dash lines: $p < 0.001$).

(H) GCaMP6 responses by 920nm two-photon activation of ReaChR in cells with and without the expression of tdTomato. Curve fitting showed that tdTomato-expressing neurons are more efficiently activated than tdTomato-negative neurons at various laser powers (20% rise of GCaMP6 fluorescence used as arbitrary threshold of neuronal activation) ($p = 0.0015$ comparing differences between fitted curves, see STAR Methods for statistical details).

DISCUSSION

Here, we reported a novel approach to improve the limited efficiency of two-photon illumination for opsin stimulation *in vivo*. By positioning organic dyes or genetically encoded fluorescent proteins in the cytoplasm or immediate vicinity of opsins (intravascular), and using

two-photon illumination to excite them, a focal source of single-photon emissions is generated, which efficiently activates adjacent opsins. We demonstrated that TEFT improves the efficiency of *in vivo* experiments otherwise not easily achievable with widely available standard two-photon microscopy setups. This is particularly evident when using optogenetic stimulation of brain vasculature to study mural cell contractility and the control of neurovascular coupling. For example, a recent study applied two-photon optogenetic stimulation to induce single vessel segment constriction using spatial light modulator at much higher laser power[42] compared to that used in our study.

TEFT retains the focal illumination properties (given the rapid intensity decay as a function of distance from the single-photon light source, see Figure 1). This allows opsin stimulation at cellular and possibly subcellular resolution, given our calculations showing that TEFT has a low (<14%) crosstalk illumination power to neighboring cells (Figures 1 and S4). Together with the fact that the effective illumination power is higher in smaller structures (inversely correlated with surface area, Figure 1), TEFT could provide a potent method for optogenetic experiments requiring high resolution such as those of single dendritic spines. In addition, the lower laser power requirements achieved by this method could be important for reducing thermal injury[43] and unwanted laser-induced electrophysiological effects independent of opsin activation.[14,16] Altogether, our study introduces a significant improvement in the methodologies for targeted cell optogenetics stimulation that are critical for experiments requiring precise spatial and temporal single-cell stimulation for investigation of brain physiology and neural networks *in vivo*.

Limitations of the study

First, TEFT could be further optimized in the future by improving the quantum yield of the paired fluorescent proteins utilized. Importantly, one can also control the concentration of either small fluorophores or fluorescent proteins and their location (i.e., cell cytoplasm or intravascular space) and excite the full volume of the PSF which is much greater than the amount of membrane bound opsins that are normally excited by direct two-photon illumination. Second, we mainly use fluorophores or organic dyes as a medium for converting two-photon excitation light but the source of fluorescence can be extended to light-emitting nanoparticles and use near-infrared light in combination with optogenetic techniques to reach deeper brain areas.[44] Finally, this method is entirely compatible and should also improve the efficiency of other methods for two-photon optogenetic stimulation such as the use of fast spiral scanning paths[4,9] or scanless holographic approaches.[22,23]

STAR★METHODS

Detailed methods are provided in the online version of this paper and include the following:

- KEY RESOURCES TABLE
- RESOURCE AVAILABILITY
  - Lead contact
  - Materials availability
  - Data and code availability
- EXPERIMENTAL MODEL AND STUDY PARTICIPANT DETAILS
  - Mice
- METHOD DETAILS
  - Reagents
  - In utero electroporation
  - Craniotomy surgery, window implantation and *in vivo* two-photon imaging
  - Single cell patch clamp and two-photon optogenetics
  - Simulation of the TEFT effect
- QUANTIFICATION AND STATISTICAL ANALYSIS

SUPPLEMENTAL INFORMATION

Supplemental information can be found online at https://doi.org/10.1016/j.isci.2023.107857.

ACKNOWLEDGMENTS

We thank Dr. Oscar Hernandez (Stanford University) and Dr. Bo Li (Fudan University) for their guidance on the estimation of fluorescence irradiance by two-photon excitation, and Dr. Jonathan Demb (Yale University) for helpful conceptual and technical discussions. This work was supported by NIH R01NS115544 and RO1NS111961 (J.G.). J.B. was additionally supported by NIH R01GM118486. M.C. and Z.J.Z were additionally supported by NIH R01EY026065 (ZJZ), P30EY026878 (Yale Vision Core). P.Y. was additionally supported by Shanghai Pilot Program for Basic Research – FuDan University 21TQ1400100 (22TQ019), Shanghai Municipal Science and Technology Major Project, the Lingang Laboratory (grant no. LG-QS-202203-09) and Shanghai Natural Science Foundation (22ZR1415000). W.K. was additionally supported by National Natural Science Foundation of China (Grant: 32200953). Y.S. was additionally supported by National Natural Science Foundation of China (Grant: T2241002).

AUTHOR CONTRIBUTIONS

P.Y and J.G. designed the study. L.T., P.Y., and F.C. carried out the experiments. P.Y., S.H., and J.B. performed theoretical calculations. Y.X., L.T., M.C., W.K., Y.S., N.D., and J.Z. performed the electrophysiology recording. P.Y., L.T., S.H., and J.G. wrote and edited the manuscript. J.G. and P.Y. directed the study.

DECLARATION OF INTERESTS

The authors declare no competing interests.

INCLUSION AND DIVERSITY

We support inclusive, diverse, and equitable conduct of research.

Received: April 27, 2022
Revised: June 1, 2023
Accepted: September 6, 2023
Published: September 9, 2023

REFERENCES

1. Boyden, E.S., Zhang, F., Bamberg, E., Nagel, G., and Deisseroth, K. (2005). Millisecond-timescale, genetically targeted optical control of neural activity. Nat. Neurosci. *8*, 1263–1268. https://doi.org/10.1038/nn1525.
2. Duebel, J., Marazova, K., and Sahel, J.A. (2015). Optogenetics. Curr. Opin. Ophthalmol. *26*, 226–232. https://doi.org/10.1097/ICU.0000000000000140.
3. Oron, D., Papagiakoumou, E., Anselmi, F., and Emiliani, V. (2012). Two-photon optogenetics. Prog. Brain Res. *196*, 119–143. https://doi.org/10.1016/B978-0-444-59426-6.00007-0.
4. Prakash, R., Yizhar, O., Grewe, B., Ramakrishnan, C., Wang, N., Goshen, I., Packer, A.M., Peterka, D.S., Yuste, R., Schnitzer, M.J., and Deisseroth, K. (2012). Two-photon optogenetic toolbox for fast inhibition, excitation and bistable modulation. Nat. Methods *9*, 1171–1179. https://doi.org/10.1038/nmeth.2215.
5. Carrillo-Reid, L., Yang, W., Bando, Y., Peterka, D.S., and Yuste, R. (2016). Imprinting and recalling cortical ensembles. Science (New York, N.Y.) *353*, 691–694. https://doi.org/10.1126/science.aaf7560.
6. Shemesh, O.A., Tanese, D., Zampini, V., Linghu, C., Piatkevich, K., Ronzitti, E., Papagiakoumou, E., Boyden, E.S., and Emiliani, V. (2017). Temporally precise single-cell-resolution optogenetics. Nat. Neurosci. *20*, 1796–1806. https://doi.org/10.1038/s41593-017-0018-8.
7. Mardinly, A.R., Oldenburg, I.A., Pégard, N.C., Sridharan, S., Lyall, E.H., Chesnov, K., Brohawn, S.G., Waller, L., and Adesnik, H. (2018). Precise multimodal optical control of neural ensemble activity. Nat. Neurosci. *21*, 881–893. https://doi.org/10.1038/s41593-018-0139-8.
8. Zhang, Z., Russell, L.E., Packer, A.M., Gauld, O.M., and Häusser, M. (2018). Closed-loop all-optical interrogation of neural circuits *in vivo*. Nat. Methods *15*, 1037–1040. https://doi.org/10.1038/s41592-018-0183-z.
9. Rickgauer, J.P., and Tank, D.W. (2009). Two-photon excitation of channelrhodopsin-2 at saturation. Proc. Natl. Acad. Sci. USA *106*, 15025–15030. https://doi.org/10.1073/pnas.0907084106.
10. Zhu, P., Narita, Y., Bundschuh, S.T., Fajardo, O., Schärer, Y.P.Z., Chattopadhyaya, B., Bouldoires, E.A., Stepien, A.E., Deisseroth, K., Arber, S., et al. (2009). Optogenetic Dissection of Neuronal Circuits in Zebrafish using Viral Gene Transfer and the Tet System. Front. Neural Circ. *3*, 21. https://doi.org/10.3389/neuro.04.021.2009.
11. Andrasfalvy, B.K., Zemelman, B.V., Tang, J., and Vaziri, A. (2010). Two-photon single-cell optogenetic control of neuronal activity by sculpted light. Proc. Natl. Acad. Sci. USA *107*, 11981–11986. https://doi.org/10.1073/pnas.1006620107.
12. Papagiakoumou, E., Anselmi, F., Bègue, A., de Sars, V., Glückstad, J., Isacoff, E.Y., and Emiliani, V. (2010). Scanless two-photon excitation of channelrhodopsin-2. Nat. Methods *7*, 848–854. https://doi.org/10.1038/nmeth.1505.
13. Denk, W., Strickler, J.H., and Webb, W.W. (1990). Two-photon laser scanning fluorescence microscopy. Science (New York, N.Y.) *248*, 73–76. https://doi.org/10.1126/science.2321027.
14. Wells, J., Kao, C., Mariappan, K., Albea, J., Jansen, E.D., Konrad, P., and Mahadevan-Jansen, A. (2005). Optical stimulation of neural tissue *in vivo*. Opt. Lett. *30*(5), 504–506. https://doi.org/10.1364/ol.30.000504.
15. Rungta, R.L., Osmanski, B.F., Boido, D., Tanter, M., and Charpak, S. (2017). Light controls cerebral blood flow in naive animals. Nat. Commun. *8*, 14191. https://doi.org/10.1038/ncomms14191.
16. Walsh, A.J., Tolstykh, G.P., Martens, S., Ibey, B.L., and Beier, H.T. (2016). Action potential block in neurons by infrared light. Neurophotonics *3*, 040501. https://doi.org/10.1117/1.NPh.3.4.040501.
17. Picot, A., Dominguez, S., Liu, C., Chen, I.W., Tanese, D., Ronzitti, E., Berto, P., Papagiakoumou, E., Oron, D., Tessier, G., et al. (2018). Temperature Rise under Two-Photon Optogenetic Brain Stimulation. Cell Rep. *24*, 1243–1253.e5. https://doi.org/10.1016/j.celrep.2018.06.119.
18. Owen, S.F., Liu, M.H., and Kreitzer, A.C. (2019). Thermal constraints on *in vivo* optogenetic manipulations. Nat. Neurosci. *22*, 1061–1065. https://doi.org/10.1038/s41593-019-0422-3.
19. Davalos, D., Grutzendler, J., Yang, G., Kim, J.V., Zuo, Y., Jung, S., Littman, D.R., Dustin, M.L., and Gan, W.B. (2005). ATP mediates rapid microglial response to local brain injury *in vivo*. Nat. Neurosci. *8*, 752–758. https://doi.org/10.1038/nn1472.
20. Zeng, X.C., Bhasin, S., Wu, X., Lee, J.G., Maffi, S., Nichols, C.J., Lee, K.J., Taylor, J.P., Greene, L.E., and Eisenberg, E. (2004). Hsp70 dynamics *in vivo*: effect of heat shock and protein aggregation. J. Cell Sci. *117*, 4991–5000. https://doi.org/10.1242/jcs.01373.
21. Duke, C.G., Savell, K.E., Tuscher, J.J., Phillips, R.A., 3rd, and Day, J.J. (2020). Blue Light-Induced Gene Expression Alterations in Cultured Neurons Are the Result of Phototoxic Interactions with Neuronal Culture Media. eNeuro *7*. ENEURO.0386-19.2019. https://doi.org/10.1523/ENEURO.0386-19.2019.
22. Hernandez, O., Papagiakoumou, E., Tanese, D., Fidelin, K., Wyart, C., and Emiliani, V. (2016). Three-dimensional spatiotemporal focusing of holographic patterns. Nat. Commun. *7*, 11928. https://doi.org/10.1038/ncomms11928.
23. Pégard, N.C., Mardinly, A.R., Oldenburg, I.A., Sridharan, S., Waller, L., and Adesnik, H. (2017). Three-dimensional scanless holographic optogenetics with temporal focusing (3D-SHOT). Nat. Commun. *8*, 1228. https://doi.org/10.1038/s41467-017-01031-324.
24. Carrillo-Reid, L., Han, S., Yang, W., Akrouh, A., and Yuste, R. (2019). Controlling visually guided behavior by holographic recalling of cortical ensembles. Cell *178*, 447–457.e5. https://doi.org/10.1016/j.cell.2019.05.045.
25. Marshel, J.H., Kim, Y.S., Machado, T.A., Quirin, S., Benson, B., Kadmon, J., Raja, C., Chibukhchyan, A., Ramakrishnan, C., Inoue, M., et al. (2019). Cortical layer-specific critical dynamics triggering perception. Science (New York, N.Y.) *365*, eaaw5202. https://doi.org/10.1126/science.aaw5202.
26. Rickgauer, J.P., Deisseroth, K., and Tank, D.W. (2014). Simultaneous cellular-resolution optical perturbation and imaging of place cell firing fields. Nat. Neurosci. *17*, 1816–1824. https://doi.org/10.1038/nn.3866.
27. Packer, A.M., Russell, L.E., Dalgleish, H.W.P., and Häusser, M. (2015). Simultaneous all-optical manipulation and recording of neural circuit activity with cellular resolution *in vivo*. Nat. Methods *12*, 140–146. https://doi.org/10.1038/nmeth.3217.

28. Lin, J.Y., Knutsen, P.M., Muller, A., Kleinfeld, D., and Tsien, R.Y. (2013). ReaChR: a red-shifted variant of channelrhodopsin enables deep transcranial optogenetic excitation. Nat. Neurosci. *16*, 1499–1508. https://doi.org/10.1038/nn.3502.
29. Chaigneau, E., Ronzitti, E., Gajowa, M.A., Soler-Llavina, G.J., Tanese, D., Brureau, A.Y.B., Papagiakoumou, E., Zeng, H., and Emiliani, V. (2016). Two-Photon Holographic Stimulation of ReaChR. Front. Cell. Neurosci. *10*, 234. https://doi.org/10.3389/fncel.2016.00234.
30. Webb, R.C. (2003). Smooth muscle contraction and relaxation. Adv. Physiol. Educ. *27*, 201–206. https://doi.org/10.1152/advan.00025.2003.
31. Hill, R.A., Tong, L., Yuan, P., Murikinati, S., Gupta, S., and Grutzendler, J. (2015). Regional Blood Flow in the Normal and Ischemic Brain Is Controlled by Arteriolar Smooth Muscle Cell Contractility and Not by Capillary Pericytes. Neuron *87*, 95–110. https://doi.org/10.1016/j.neuron.2015.06.001.
32. Mateo, C., Knutsen, P.M., Tsai, P.S., Shih, A.Y., and Kleinfeld, D. (2017). Entrainment of Arteriole Vasomotor Fluctuations by Neural Activity Is a Basis of Blood-Oxygenation-Level-Dependent "Resting-State" Connectivity. Neuron *96*, 936–948.e3. https://doi.org/10.1016/j.neuron.2017.10.012.
33. Hartmann, D.A., Berthiaume, A.A., Grant, R.I., Harrill, S.A., Koski, T., Tieu, T., McDowell, K.P., Faino, A.V., Kelly, A.L., and Shih, A.Y. (2021). Brain capillary pericytes exert a substantial but slow influence on blood flow. Nat. Neurosci. *24*, 633–645. https://doi.org/10.1038/s41593-020-00793-2.
34. Tong, L., Hill, R.A., Damisah, E.C., Murray, K.N., Yuan, P., Bordey, A., and Grutzendler, J. (2021). Imaging and optogenetic modulation of vascular mural cells in the live brain. Nat. Protoc. *16*, 472–496. https://doi.org/10.1038/s41596-020-00425-w.
35. Mohanty, S.K., Reinscheid, R.K., Liu, X., Okamura, N., Krasieva, T.B., and Berns, M.W. (2008). In-depth activation of channelrhodopsin 2-sensitized excitable cells with high spatial resolution using two-photon excitation with a near-infrared laser microbeam. Biophys. J. *95*, 3916–3926. https://doi.org/10.1529/biophysj.108.130187.
36. Han, X., Chow, B.Y., Zhou, H., Klapoetke, N.C., Chuong, A., Rajimehr, R., Yang, A., Baratta, M.V., Winkle, J., Desimone, R., and Boyden, E.S. (2011). A high-light sensitivity optical neural silencer: development and application to optogenetic control of non-human primate cortex. Front. Syst. Neurosci. *5*, 18. https://doi.org/10.3389/fnsys.2011.00018.
37. Chen, T.W., Wardill, T.J., Sun, Y., Pulver, S.R., Renninger, S.L., Baohan, A., Schreiter, E.R., Kerr, R.A., Orger, M.B., Jayaraman, V., et al. (2013). Ultrasensitive fluorescent proteins for imaging neuronal activity. Nature *499*, 295–300. https://doi.org/10.1038/nature12354.
38. Drobizhev, M., Makarov, N.S., Tillo, S.E., Hughes, T.E., and Rebane, A. (2011). Two-photon absorption properties of fluorescent proteins. Nat. Methods *8*, 393–399. https://doi.org/10.1038/nmeth.1596.
39. Drobizhev, M., Tillo, S., Makarov, N.S., Hughes, T.E., and Rebane, A. (2009). Absolute two-photon absorption spectra and two-photon brightness of orange and red fluorescent proteins. J. Phys. Chem. B *113*, 855–859. https://doi.org/10.1021/jp8087379.
40. Lin, J.Y. (2011). A user's guide to channelrhodopsin variants: features, limitations and future developments. Exp. Physiol. *96*, 19–25. https://doi.org/10.1113/expphysiol.2009.051961.
41. Cherkas, V., Grebenyuk, S., Osypenko, D., Dovgan, A.V., Grushevskyi, E.O., Yedutenko, M., Sheremet, Y., Dromaretsky, A., Bozhenko, A., Agashkov, K., et al. (2018). Measurement of intracellular concentration of fluorescently-labeled targets in living cells. PLoS One *13*, e0194031. https://doi.org/10.1371/journal.pone.0194031.
42. O'Herron, P.J., Hartmann, D.A., Xie, K., Kara, P., and Shih, A.Y. (2022). 3D optogenetic control of arteriole diameter *in vivo*. Elife *11*, e72802. https://doi.org/10.7554/eLife.72802.
43. Yang, W., Carrillo-Reid, L., Bando, Y., Peterka, D.S., and Yuste, R. (2018). Simultaneous two-photon imaging and two-photon optogenetics of cortical circuits in three dimensions. Elife *7*, e32671. https://doi.org/10.7554/eLife.32671.
44. Chen, S., Weitemier, A.Z., Zeng, X., He, L., Wang, X., Tao, Y., Huang, A.J.Y., Hashimotodani, Y., Kano, M., Iwasaki, H., et al. (2018). Near-infrared deep brain stimulation via upconversion nanoparticle-mediated optogenetics. Science (New York, N.Y.) *359*, 679–684. https://doi.org/10.1126/science.aaq1144.
45. Chen, F., and LoTurco, J. (2012). A method for stable transgenesis of radial glia lineage in rat neocortex by piggyBac mediated transposition. J. Neurosci. Methods *207*, 172–180. https://doi.org/10.1016/j.jneumeth.2012.03.016.
46. Hill, R.A., Damisah, E.C., Chen, F., Kwan, A.C., and Grutzendler, J. (2017). Targeted two-photon chemical apoptotic ablation of defined cell types *in vivo*. Nat. Commun. *8*, 15837. https://doi.org/10.1038/ncomms15837.
47. Ting, J.T., Lee, B.R., Chong, P., Soler-Llavina, G., Cobbs, C., Koch, C., Zeng, H., and Lein, E. (2018). Preparation of Acute Brain Slices Using an Optimized N-Methyl-D-glucamine Protective Recovery Method. J. Vis. Exp.53825 https://doi.org/10.3791/53825.
48. Mütze, J., Iyer, V., Macklin, J.J., Colonell, J., Karsh, B., Petrášek, Z., Schwille, P., Looger, L.L., Lavis, L.D., and Harris, T.D. (2012). Excitation spectra and brightness optimization of two-photon excited probes. Biophys. J. *102*, 934–944. https://doi.org/10.1016/j.bpj.2011.12.056.
49. Xu, C., and Webb, W.W. (2002). Multiphoton Excitation of Molecular Fluorophores and Nonlinear Laser Microscopy. In Topics in Fluorescence Spectroscopy, *vol 5*, J.R. Lakowicz, ed. Topics in Fluorescence Spectroscopy (Springer). https://doi.org/10.1007/0-306-47070-5_11.
50. Zipfel, W.R., Williams, R.M., and Webb, W.W. (2003). Nonlinear magic: multiphoton microscopy in the biosciences. Nat. Biotechnol. *21*, 1369–1377. https://doi.org/10.1038/nbt899.
51. Schindelin, J., Arganda-Carreras, I., Frise, E., Kaynig, V., Longair, M., Pietzsch, T., Preibisch, S., Rueden, C., Saalfeld, S., Schmid, B., et al. (2012). Fiji: an open-source platform for biological-image analysis. Nat. Methods *9*, 676–682. https://doi.org/10.1038/nmeth.2019.
52. Quinn, P., Griffiths, G., and Warren, G. (1984). Density of newly synthesized plasma membrane proteins in intracellular membranes II. Biochemical studies. J. Cell Biol. *98*, 2142–2147. https://doi.org/10.1083/jcb.98.6.2142.
53. Nagel, G., Möckel, B., Büldt, G., and Bamberg, E. (1995). Functional expression of bacteriorhodopsin in oocytes allows direct measurement of voltage dependence of light induced H+ pumping. FEBS Lett. *377*, 263–266. https://doi.org/10.1016/0014-5793(95)01356-3.

STAR★METHODS

KEY RESOURCES TABLE

REAGENT or RESOURCE	SOURCE	IDENTIFIER
Chemicals, peptides, and recombinant proteins		
Bovine Serum Albumin	Sigma-Aldrich	05470; CAS: 9048-46-8
Cascade Blue™ Acetyl Azide, Trisodium Salt	Thermo Fisher Scientific	C2284
AMCA-X Succinimidyl Ester	Thermo Fisher Scientific	A6118
Alexa Fluor™ 405 NHS Ester (Succinimidyl Ester)	Thermo Fisher Scientific	A30000
Lucifer Yellow iodoacetamide, Dipotassium Salt	Thermo Fisher Scientific	L1338
Experimental models: Organisms/strains		
Mouse: B6;FVB-*Ifi*208$^{Tg(Cspg4\text{-}cre)1Akik}$/J	The Jackson Laboratory	JAX# 008533, RRID:IMSR_JAX:008533
Mouse: Ai40(RCL-ArchT/EGFP)-D	The Jackson Laboratory	JAX# 021188, RRID: IMSR_JAX:021188
Mouse: Ai32(RCL-ChR2(H134R)/EYFP)	The Jackson Laboratory	JAX# 012569, RRID:IMSR_JAX:012569
Mouse: BALB/Cj	The Jackson Laboratory	JAX# 000651, RRID:IMSR_JAX:000651
Recombinant DNA		
Plasmid: CAG-tdTomato	Addgene	#83029
Plasmid: CAG-ReaChR	Addgene	#50954
Plasmid: Syn-GCaMP6f	Addgene	#100837
Plasmid: CAG-tagBFP	Addgene	#49151
Plasmid: Syn-ChR2	Addgene	#58880
Plasmid: CAG-jRCaMP	Addgene	#61562
Software and algorithms		
GraphPad Prism (8.4.1)	GraphPad Software	https://www.graphpad.com
Prairie View software	Bruker	N/A
MaiTai software	MaiTai Technologies	N/A
Matlab 2019b	MathWorks	www.mathworks.com
ImageJ	Schindelin et al., 2012[51]	https://imagej.net/ij/

RESOURCE AVAILABILITY

Lead contact

Further information and requests for data should be directed to and will be fulfilled by the lead contact. Jaime Grutzendler, Department of Neuroscience, Yale School of Medicine, New Haven, CT, 06511, 203-737-2765, jaime.grutzendler@yale.edu.

Materials availability

This study did not generate new unique reagents.

Data and code availability

- All data reported in this paper will be shared by the lead contact upon request.
- All original code is available in this paper's supplemental information.
- Any additional information required to reanalyze the data reported in this paper is available from the lead contact upon request.

EXPERIMENTAL MODEL AND STUDY PARTICIPANT DETAILS

Mice

All rodent procedures were approved by the Yale University Institutional Animal Care and Use Committee. For vascular studies, transgenic mice that express the Cre recombinase under the mural cell NG2 (Cspg4) promoter, and reporter lines with cre-dependent channelrhodopsin-2 (Ai32) or Archaerhodopsin-3 (Ai40D) were purchased from The Jackson Laboratory (JAX# 008533, JAX# 021188, JAX# 012569). Cre-expressing strains were crossbred with the reporter strains and the offspring were used for all experiments. For neuronal studies, wild type mice were used for electroporation of various constructs (JAX# 000651). All mice were not involved in pervious procedures and were tested naïve. All subjects were housed on a 12-h/12-h light/dark cycle in a 22–24°C environment. For all experiments, 2-3-month-old mice from both sexes were used, no effect of gender was observed in the experiment. The number of mice used for each experiment were labeled in figure legends.

METHOD DETAILS

Reagents

Purified albumin (Sigma-Aldrich, 05470) was used for fluorescent dye conjugation. Reactive esters were used for labeling (Thermo Fisher Scientific, C-2284, A6118, A30000, L-1338) according to the manufacturer's instruction. The labeled albumin was diluted so that 5mg reactive dyes constituted 1mL of injection stock. 100μl of labeled albumin was injected intravenously before imaging, final dye concentration in blood was estimated to be ~0.5mM. In all conjugations, albumin was used at concentrations greater than the number of fluorophores to eliminate the need for free fluorophore purification.

To express constructs by *in Utero* electroporation we obtained and modified the following plasmid constructs from Addgene: CAG-tdTomato, CAG-ReaChR (#50954), Syn-GCaMP6f (#100837), CAG-tagBFP (#49151), Syn-ChR2 (#58880), CAG-jRCaMP (#61562). The DNA sequences encoding the target proteins (tagBFP, tdTomato and ReaChR) were cloned from the original constructs into an AAV-CAG backbone (the backbone was acquired from Addgene #28014, deleting the GFP sequence), and the resulted plasmids were used for *in utero* electroporation. Standard molecular cloning procedures were performed using the following reagents: Phusion High-Fidelity DNA Polymerase (New England BioLabs, M0530S), Restriction enzymes (New England BioLabs), T4 DNA ligase (ThermoFisher Scientific, EL0011), QIAGEN plasmid Maxi kit (#12162). All modified constructs were sequences to verify the correct insertion and sequence.

In utero electroporation

In utero electroporation was done as previously described.[45] Briefly, Plasmids were used at the final concentration of 1.0 μg/μl (for each plasmid), mixed with 2 mg/ml Fast Green for visualization during plasmid injection and electroporation. Electroporation was performed around embryonic day 13 to 15 (E13 to E15). Mice were anesthetized with ketamine/xylazine (100mg/kg and 10mg/kg i.p.). Buprenorphine was administered (i.p.) every 12 hours for 2 more days following surgery. After exposing the uterine horns, ~1 μl of plasmid mixture was pressure injected into the lateral ventricle of each embryo via a pulled glass microelectrode (tip size 10~20 um) using Picospritzer II (General Valve, 20 psi). 50 V current pulses generated by a BTX 8300 pulse generator (BTX Harvard Apparatus) were used for electroporation. Mice were allowed to age to 1 month prior to utilization in all experiments.

In order to verify the co-expression of tdTomato, ReaChR and GCaMP6, we used *in vivo* two-photon imaging to monitor the cells while shining a red LED to trigger ReaChR activation, triple positive cells should have baseline red fluorescent signal and a LED-triggered green fluorescent signal. The co-expression probability was very high with electroporation. And only cells that demonstrated robust triple expression were then targeted for two-photon stimulation.

Craniotomy surgery, window implantation and *in vivo* two-photon imaging

Mice were anesthetized with an intraperitoneal injection of Ketamine/Xylazine mixture, with final concentration of 100mg/kg and 10mg/kg, respectively. The status of anesthesia was assessed periodically with hind paw pinch. The mouse was head-fixed to a custom-made headplate by gluing the skull to it. A craniotomy of about 4mm diameter was made (AP -1.5mm, ML 2.0 mm) with a dental drill, with dura mater carefully removed. A coverslip was put to cover the craniotomy opening and secured with cyanoacrylate glue. The mouse was kept anesthetized during subsequent imaging sessions, and immediately euthanized after finalizing the experiment.

Two-photon imaging was carried out with a commercial system (Bruker Ultima Investigator), controlled through Prairie View software. A tunable Ti:Sapphire laser was used to generate two-photon excitation with its wavelength and mode-locking tuned through MaiTai software. In the case of RCaMP imaging, a 1045nm fixed wavelength laser (MaiTai InSight X3) was used. A pockels cell was used to modulate laser power; and the laser power on the sample was measured with a power meter (Thorlabs PM100D). The point scanning was achieved by galvanometer scanners with various dwell times. The full frame rate was kept at 0.5 Hz, and for stimulation, the scanning within regions of interests (ROIs) was at 20 Hz or 50 Hz frequencies. During ROI scanning, the regions outside the ROI were not scanned nor imaged (represented by the dashed portion of the GCaMP6 response curved in Figure 3). Fluorescence emission was collected with gallium arsenide phosphide photomultiplier tubes. A 20x water immersion 1.0 numerical aperture objective (Zeiss) and a 10x air 0.4 numerical aperture objective (Leica) were used for most experiments. For all in-vivo experiments, imaged blood-vessels were identified within 250 μm from pia mater, and imaged neurons were located at depth between 100 to 350 μm. In all our experiments, cells demonstrated normal spontaneous and stimulated responses, and showed no signs of persistently elevated calcium levels associated with cell damage.[46]

Single cell patch clamp and two-photon optogenetics

Acute brain slices of the *in utero* electroporated mice (P30-P40) were prepared following a N-methyl-D-glucamine (NMDG) protective recovery method.[47] Whole cell patch clamp and two-photon optogenetics were then performed in slices in an ASCF containing (in mM) 120 NaCl, 3.1 KCl, 1.1 CaCl2, 1.2 MgCl2, 1.25 MgSO4,26 NaHCO3, 0.5 L-glutamine, 0.1 ascorbic acid, 0.1 Na-pyruvate, and 20 glucose; saturated with 95% O2–5% CO2 at 35°C. To target fluorescent cells, we used a two-photon microscope system (Ultima; Prairie Technologies) equipped with a Ti:Sapphire pulsed laser (MaiTai), configured on an Olympus upright microscope (BX51WI) with a 20×, 0.5 NA objective lens (LUMPlanFL/IR) and a 60x, 1.0 NA objective lens(LUMPLANFL/IR). Cells were patched under 60x objective lens with pipette solutions as follows (in mM): (1) for voltage clamp, 105 CsMeSO4, 0.5 CaCl2,10 HEPES, 5 EGTA, 5 Na2-phosphocreatine, 2 ATP-Mg, 0.5 GTP-2Na, 2 ascorbic acid, and 8 QX314-Cl (pH 7.2), with 20–30 CsOH; (2) for current clamp, 105 potassium gluconate, 5 KCl, 0.5 CaCl2, 2 MgCl2, 5 EGTA, 10 HEPES, 5 Na2-phosphocreatine, 2 ATP-2Na, 0.5 GTP-2Na, and 2 ascorbic acid (pH 7.2) with 5 NaOH and 15 KOH. Liquid junction potential was calculated with pCLAMP software and corrected (Molecular Devices, Union City, CA). Once whole cell patch clamp was achieved, 20x objective lens was switched for two-photon optogenetics. A single ROI (~10 x 10 μm) including only the cell soma was chosen for raster scan, with 4 μs dwell time, and laser intensity less than 25 mW (3.8, 5.4, 7.3, 8.9, 12, 14.8, 18.1 and 21.6 mW), which shows no clear photo damage to cell membranes. 800 nm wavelength was used to excite intracellular dye (Alexa 594, 0.5 mM). The photocurrent under 920 nm, which would not activate Alexa 594[48] was also recorded to evaluate the expression level of ReaChR. An external voltage was used to trigger the two-photon image scan, so that the timing of laser scanning and cell voltage/current can be accurately matched for later analysis. The raster scanning was started at 0.1 s in each trail and last for 50 ms.

Simulation of the TEFT effect

The algebraic calculation of TEFT effect was carried out in MATLAB, following the equations described in Figures 1 and S4. Here we provide an additional discussion regarding whether the red fluorescent protein commonly fused with opsins would be a potent TEFT source, as this question has been brought up multiple times from several readers. The dense packing of fluorescent proteins is a key factor for the efficiency of the TEFT method. Thus, in the case of fusion protein, the 1:1 ratio between opsin and fluorphore and their location on the membrane both limit the generation of sufficient photons. To illustrate this point, here we described a back-of-envelope calculation to put this into proper scale. The key issue is that a fusion protein cannot provide enough photons to induce the TEFT effect.

For TEFT illumination, we used the parameters described in Figure 1:

Two-photon focal volume: 0.28×10^{-15} L, fluorophore concentration: 10 μM, this leads to a total of 1686 molecules stimulated at each pulse of two-photon excitation.

Number of molecules = focal volume x concentration x Avogadro's number = $0.28 \times 10^{-15} \times 10 \times 10^{-6} \times 6.02 \times 10^{23} \approx 1686$

For membrane fusion, the expression of opsins can be ranging from 90 - 750 molecules per μm.[2,52,53] Given the ~0.2 μm XY-plane resolution, the activated molecules on the membrane are fewer than 30, which is about 2 orders of magnitude lower than the TEFT methods. In fact, the estimated total density of membrane proteins is about 30000 molecules per μm^2, and usually the overexpression of exogenous proteins will be ~2-3 % of this value. Even if we are assuming very generously that the opsin expression constitutes 10% of total membrane protein, which is never achieved, we are still only activating ~120 molecules at each moment, which is one order of magnitude lower than the TEFT method.

QUANTIFICATION AND STATISTICAL ANALYSIS

Statistical analyses were carried out using GraphPad Prism (8.4.1). Data were presented in mean ± standard deviation in Figure 2, and in mean ± standard error in Figure S4. For comparing normalized vessel diameter time-lapse traces (Figures 2D and 2I), Student's t-test was performed with each timepoint, with Bonferroni correction for multiple comparison. For comparing the two-photon mediated vessel motility in different conditions, one-sample Wilcoxon tests were used for each group to compare to a value of 1 (Figures 2E and 2J) or 0 (Figure 2F), with additional Bonferroni's correction for multiple comparison. For comparing the efficacy of neuronal optogenetics with and without fluorescence transfer (Figure S4E), we fit the response probability from each group to the following exponential equation: Y = 1-exp(-K*(X-L), in which the parameter L indicates the minimal power to elicit calcium responses and K indicates the change rate of the curve. Extra sum-of-squares F test was used to determine whether two sets of parameters were statistically different.